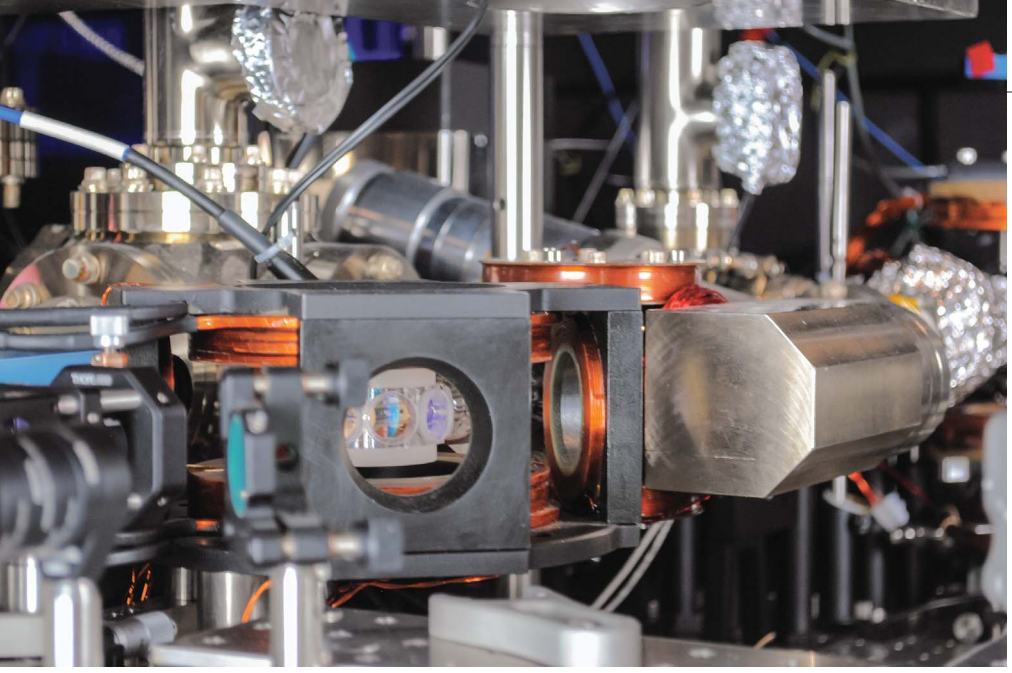

PHOTO: L. DE MARCO

The experimental apparatus and the supporting optical components for the production and manipulation of a quantum gas of polar molecules (KRb).

REVIEW

Cold molecules: Progress in quantum engineering of chemistry and quantum matter

John L. Bohn,* Ana Maria Rey,* Jun Ye*

Cooling atoms to ultralow temperatures has produced a wealth of opportunities in fundamental physics, precision metrology, and quantum science. The more recent application of sophisticated cooling techniques to molecules, which has been more challenging to implement owing to the complexity of molecular structures, has now opened the door to the longstanding goal of precisely controlling molecular internal and external degrees of freedom and the resulting interaction processes. This line of research can leverage fundamental insights into how molecules interact and evolve to enable the control of reaction chemistry and the design and realization of a range of advanced quantum materials.

Molecules hold a central place in the physical sciences. On the one hand, molecules consisting of a small number of atoms represent the upper limit of complexity that we can hope at present to understand in complete detail, starting from quantum mechanics. On the other hand, molecules are the building blocks from which more complex phenomena emerge, including chemistry, condensed matter, and life itself. Molecules then represent a kind of intellectual fulcrum around which we can leverage our complete understanding of small systems to probe and manipulate increasingly complex ones.

Precisely controlled studies of molecules started decades ago, with the invention of supersonic molecular beams for cooling (*1*) and coherent control for manipulation of internal states (*2*). However, bringing the temperature of molecular gases to the quantum regime is a relatively recent endeavor (*3*). When molecules move extremely slowly in the laboratory frame, and control of their internal degrees of freedom is achieved at the level of individual quantum states, then each step of a complex chemical reaction can in principle be monitored and measured. The energy resolution underpinning such a process would be limited only by fundamental quantum rules that govern the molecular interaction from start to finish. The capability to track in full detail how multiple molecular species approach each other, interact through their evolving potential energy landscape, form intermediates, and reemerge as final products, all while monitoring the internal and external energy-level distributions, may have seemed out of reach only a few years ago. However, thanks to the recent progress in the field of cold molecules, we could soon be able to do precisely that. First-principles understanding of the most fundamental molecular reaction processes will furthermore enable the design and control of complex molecular transformations and materials with powerful functionality.

Owing to their vibrational and rotational degrees of freedom, molecules have complex energy-level structures compared with those of atoms. This presents a challenge for cooling technology. However, once we gain control over these molecular degrees of freedom, we create opportunities to take advantage of their distinctive properties, such as precise manipulation of long-range interactions mediated by molecular electric dipole moments. This capability will enable exploration of emergent collective phenomena in interacting many-body systems, which represents one of the central challenges in science. In addition to studying chemical reactions in the new quantum regime, we may use cold molecules to synthesize quantum materials with strong correlations that could shed light on poorly understood phenomena such as superconductivity, quantum magnetism, and topological order.

Ultracold atoms have already played a revolutionary role in scientifically bridging simple quantum systems and many-body physics. Synthetic materials assembled with ultracold atoms are typically less dense than electronic materials by a factor of billions, with constituents many thousands of times heavier than electrons. These systems need to be cooled to nanokelvin temperatures before collective quantum effects start to emerge, leading to complex phenomena that are qualitatively similar to those found in real electronic materials. Low energy scales can provide advantages, such as observability in real time, but they also impose new challenges. We can overcome some of the challenges with polar molecules, because their strong and long-range interactions mitigate the requirement of cooling to ultralow motional energies.

Precise control of molecular states and the corresponding interactions is thus of paramount importance. Achieving this capability will allow us to understand chemical processes on the most fundamental, quantum mechanical bases and thus facilitate control of both coherent and dissipative molecular interaction processes. Full molecule control will also help in constructing molecule-based synthetic quantum matter to study strongly correlated quantum phenomena. Our aim here is to show how cold molecules provide the underlying connection between these different intellectual pursuits.

Chemical physics

The theme of chemical physics is to understand and eventually control how reactants become products. The idea of completely controlling and probing chemical reactions encompasses several goals, as illustrated in Fig. 1. First, reactant molecules should be prepared in individual internal quantum states, having, for instance, well-defined quantum numbers of electronic excitation, vibration,

JILA, National Institute of Standards and Technology and University of Colorado Boulder, Boulder, CO 80309-0440, USA.
*Corresponding author. Email: bohn@murphy.colorado.edu (J.L.B.); arey@jilau1.colorado.edu (A.M.R.); ye@jila.colorado.edu (J.Y.)

rotation, orientation, and alignment. In cases where it is relevant, control over electronic spin and perhaps even nuclear spin degrees of freedom of the reactants is also desirable. In addition, the collision itself should be initiated by manipulating the distribution of relative velocities of the colliding reactants. The second goal of control and probing is to measure the species constituting the products, as well as their populations in their own electronic, vibrational, rotational, and spin degrees of freedom. Relative velocities of the products are distributed according to differential cross sections—that is, angular distributions of products, which carry information about the interaction process. A final goal, and surely the most ambitious one, would be to observe, or even manipulate, the atomic complex formed during the reaction. A strong focus of this effort would be to identify transition states, in terms of their energies and atomic configurations, the barriers between them, and perhaps even the time evolution from one transition state to the next along the reaction path. Recent progress in achieving these goals has been substantial, and in some cases astonishing, as we highlight below.

State preparation and readout are largely spectroscopic procedures and can therefore be accomplished with high precision. They are assisted, moreover, by the well-controlled velocity distributions produced by molecular beams. These abilities have already led to a large and rich literature on state-to-state chemical reaction studies, described in reviews and textbooks (*4*, *5*). Under ordinary circumstances, these experiments resolve vibrational and rotational states, with tunable translational kinetic energy distributions at fractions of electron volts, suitable for probing reaction barriers.

It is not our intention to revisit this vast field, but rather to explore its extension to ever finer spectroscopic resolution and far lower translational energies. Cold molecules cover a range of temperatures, usually from a few kelvins to a few millikelvins. Ultracold refers to the regime wherein collisional processes require explicit quantum mechanical treatment (*6*). The field of cold molecule studies is large by now and has already produced many insights and developments, of which we will only highlight a few by way of illustrating some main ideas. More comprehensive reviews are available that encompass further studies [for example, (*7*–*11*)].

We therefore emphasize the situation where, beyond vibrations and rotations, fine structure and hyperfine structures are also resolved and can play a role in scattering dynamics. By considering translational temperatures on the submillikelvin scale, research arrives in a regime where collision energies are the smallest energies of the problem. At the very lowest temperatures, effects are seen that resolve individual partial waves of scattering. Lastly, the attainment of extremely slow molecules opens opportunities for manipulating the initialization of chemical reactions, beyond those afforded by conventional molecular beams.

It may seem counterintuitive that chemistry can be a subject of study at all at temperatures that are orders of magnitude below typical reaction barriers. Nevertheless, the seminal (theoretical) work of Balakrishnan and Dalgarno (*12*) showed that the rate of a chemical reaction can be considerable at zero temperature. This effect, studied first in the $F + H_2 \rightarrow H + HF$ reaction, is due to a van der Waals resonance near the threshold, which facilitates tunneling through the reaction barrier. At sufficiently low temperatures, when the de Broglie wavelength of relative motion of the reactants exceeds the range of their interaction, reaction rate constants become independent of energy, as described by the Wigner threshold law (*6*), rather than dropping as they do at higher temperatures, governed by the law of Arrhenius. Control of reactants is then a means of manipulating the way in which the reaction barrier is breached (*13*).

Reactants

Molecules are controlled most easily before the reaction begins. The reaction itself, involving nanometer length scales, electron volt energy scales, and subpicosecond time scales, leaves little room for influencing the atoms en route. In contrast, manipulating molecular samples before they are sent off to react gives the experimenter the opportunity to do the necessary state preparation, which can have decisive consequences for reaction pathways and final products.

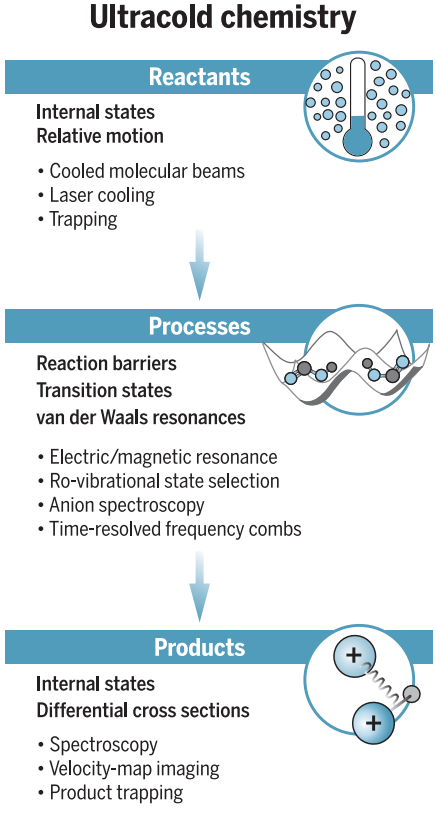

Fig. 1. Landscape of cold molecule research. Cooling enables state preparation of the reactants, precise control of the reaction process, and quantitative monitoring of the transition states and products.

The techniques of molecular state preparation reside largely in exploiting and manipulating thermodynamics. For decades, the workhorse of chemical physics has been the molecular beam, which exploits the cooling effect experienced by molecules that squirt through an aperture from a high-pressure enclosure into vacuum. This cooling process usually results in a population of molecules in very low-lying vibrational and rotational states. From here, the molecules can be state-selected or driven into the desired internal states by applied dc or radiation fields (*14*).

Molecular beams also have an impact on translational motion, producing a nonthermal distribution of velocities that has about a 10% width around its mean velocity at hundreds of meters per second in the laboratory frame. To achieve better control over the relative velocities of distinct reactants, it has long been common practice to use two such beams in a crossed configuration. Colliding the beams head-on achieves large relative velocities, whereas beams running nearly parallel have fairly low relative velocities, but a finite remaining angle limits the achievable energy resolution. The Narevicius group recently solved this long-standing problem by merging two beams perfectly in a curved magnetic guide (Fig. 2, top), achieving collision energy below 1 K (*15*).

Other techniques have emerged to slow and cool the beams in the laboratory frame. This may be done in the beam apparatus itself—for example, using the "effusive beam" technique developed by the Doyle group (*16*), wherein the beam emerges from a pressurized buffer gas of atoms that are already cold, with temperatures in the range of 2 to 20 K. This precooling mechanism, if coupled appropriately through an aperture, can produce a beam of molecules that is much slower, narrower, and better focused than a typical beam from a hot source.

Extracting a narrower subset of a beam's velocity distribution can further improve velocity resolution. Fortunately, many molecules that possess electric dipole moments respond to laboratory-strength electric fields. For example, a properly oriented ammonia molecule, moving from a field-free region "uphill" to a region of space where the electric field is 100 kV/cm, could be brought to rest from a speed of 60 m/s. Because realistic molecular velocities are higher, in practice, multiple stages of electrodes, arranged in an array termed a "Stark decelerator," are used to bring a portion of the molecules to rest in the laboratory. This technique, pioneered by the Meijer group and extended by Lewandowski, among others, has been used both as a controlled beam source (*17*–*19*) and as a means of loading molecules into electrostatic or magnetic traps, where the typical temperature is hundreds of millikelvins—a major reduction of relative velocities (*20*, *21*). In a similar vein, electrodes in a curved geometry can serve to guide sufficiently slowly moving molecules away from the main beam, isolating them from the unwanted, faster molecules (*22*).

These techniques use conservative electric potentials and therefore conserve the total phase-space density (PSD), shunting slow molecules to

GRAPHIC: ADAPTED BY N. CARY/*SCIENCE*

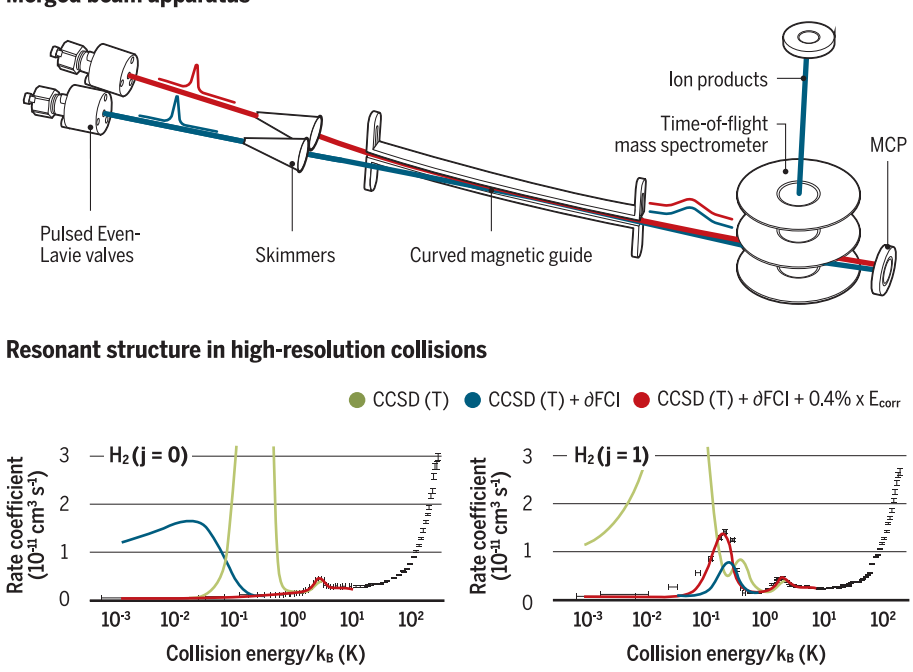

Fig. 2. High-resolution collision dynamics. (**Top**) A merged beam apparatus used for studying chemical reactions at high resolution of collision energy (below 1 K). (**Bottom**) Collisions of rotational state–selected H_2 molecules with excited (metastable) helium atoms, leading to reactive ionizations that display resonant structure as a function of collision energy. A resonance appears only if the molecule is in a rotationally excited state (right), yielding a detailed view of collision anisotropy. CCSD (T), coupled-cluster method with single, double, and approximate noniterative triple excitations; δFCI, correction arising from the full configuration interaction; E_{corr}, correlation energy; k_B, Boltzmann constant. [Adapted from (*50*, *114*) with permission]

where they are useful and throwing away the rest. The samples therefore tend to be small, although collision studies can often be usefully done (*23*). For example, an influence on the collision cross section due to dipolar interactions was observed when an electric field–guided ammonia molecular beam (produced from a buffer gas–cooled cell) collided with a magnetically trapped sample of hydroxyl radicals (produced from a Stark decelerator) (*24*). The production of cold, comparatively high-PSD samples, on the other hand, does require an actual cooling mechanism. This necessitates manipulating thermodynamics to provide a dissipative mechanism.

One such mechanism exploits the fact that the electric forces that slow a molecule are different for different internal states of the molecule. Thus, if a molecule in a high-energy state climbs a potential hill and loses kinetic energy, that kinetic energy can be permanently removed upon driving the molecule to a low-energy state, thus introducing the dissipation. For correctly chosen field configurations, this process can be cycled, ultimately lowering the molecular temperature. This mechanism has been successfully demonstrated by the Rempe group, producing cold, trapped H_2CO molecules (*25*). Another dissipative cooling process entails evaporation of trapped molecules. In the case of hydroxyl radicals trapped in a magnetic trap, a radio frequency "knife" was used to selectively remove hot molecules from a trapped to an untrapped state (*26*). The use of electric and magnetic fields together, however, leads to a severe Majorana spin flip loss mechanism (*27*), limiting the success of this approach until this problem is addressed.

A complementary technique, laser cooling, has been very successful for the field of cold atoms, though it has been a long road extending it to molecules. To bring a moving molecule to rest by means of laser cooling, the molecule needs to absorb and spontaneously emit tens of thousands of photons. However, upon the first spontaneous emission, the molecule may reside in any of a large number of rovibrational states, from which it can no longer absorb the second photon, thus ending the cycling process.

Fortunately, for a few classes of molecules, it is possible to find an excited state that decays preferentially back to a useful ground state (*28*). Combined with proper angular momentum selection rules, a magneto-optical trap (MOT) for molecules was proposed by the Ye group (*29*). The DeMille group soon reported a demonstration by laser cooling SrF molecules (*30*). This was followed by construction of a two-dimensional (2D) magneto-optic compression of YO molecules by the Ye group (*31*) and a 3D MOT of SrF by the DeMille group (*32*). Other molecular species have recently been laser-cooled as well (*33*, *34*); particularly exciting is the achievement of large numbers of CaF molecules captured in 3D MOT and sub-Doppler cooling in a 3D molasses (*35*, *36*).

Molecules can now be confined in traps constructed from spatially inhomogeneous magnetic, electric, or optical fields, including far-detuned optical dipole traps or optical lattices. Typically, the samples need to have temperatures on the order of 1 to 100 mK to be confined by laboratory magnetic or electric fields, and ultralow temperatures of a few tens of microkelvins and below for optical traps. Trapping molecules brings a completely new perspective to collisions. First, there is the substantial reduction in relative velocities, down to 0.01 to 1 m/s in favorable cases, which promises sufficient energy resolution to observe scattering resonances in chemical reactions. Second, there is a shift in perspective relative to the traditional beam approach, because the trapped molecules travel in all directions, eliminating a fixed collision axis in most cases. The concept of an impact parameter, the closest approach b between two classical trajectories in the absence of their interaction, is replaced with that of a partial wave, which better represents the quantum mechanical realities of the situation.

Moreover, in the low-energy regime achieved in traps, quantum mechanics restricts angular momentum to integer multiples of the reduced Planck constant $\hbar$. The relative angular momentum $L = \mu v b$ is conserved, where μ is the reduced mass of the colliding pair of molecules and v is their relative velocity. Thus, very roughly speaking, the available impact parameters are $b = \hbar l/\mu v$, where l = 0, 1, ... is used to index the partial wave of the collision. For zero angular momentum, "head-on" collisions with b = 0 are thus possible, and chemistry can occur. However, if the molecules possess any nonzero relative angular momentum, they are kept apart by the centrifugal potential, and the distance of closest approach increases as the energy is reduced. The question of how close together the reactants must be to initiate a possible reaction depends on the value of the constant C_6 in the long-range intermolecular interaction $-C_6/r^6$, where r is the distance between reactant molecules; this in turn defines an energy below which a given partial wave l will contribute weakly to scattering. For a light, weakly polarizable species, such as NH, this energy scale is on the order of 10 mK (*37*). Below this temperature, the colliding molecules are generally guaranteed to have no angular momentum about each other.

An ultimate goal in molecular collisions would be to extract the scattering from each partial wave—a discrete quantity—rather than having to settle for observables averaged over a continuum of impact parameters. This goal was realized in ultracold KRb molecules produced by the Jin and Ye groups (*3*, *38*–*40*). In this case, molecules were welded together optically from ultracold K and Rb atoms, ensuring a translational temperature of the molecules of ~100 nK, with the molecules in a single internal quantum state, including the absolute lowest-energy state accounting for nuclear spins. These molecules are presumably susceptible to the barrierless reaction KRb + KRb → K_2 + Rb_2, which manifested as loss in the gas, although the products were not observed.

As identical fermions in identical nuclear spin states, these molecules were forbidden by quantum mechanical symmetries from scattering via $l = 0$ partial waves and so scattered according to angular momentum $l = 1$. However, on changing the nuclear spin for half the molecules, this symmetry no longer held, and the molecules could again collide head-on with $l = 0$. Because there was no centrifugal barrier associated with this channel, the reaction rate was enhanced by almost two orders of magnitude. This was therefore the first instance of choosing the partial wave degree of freedom in relative motion, thus completing the task of controlling the reactants at all possible degrees of freedom of the collision. Further control of the molecules could be implemented by engineering the spatial configuration of the trap to restrict molecular motions in low spatial dimensions (*41*) and by introducing external fields to control the molecular orientation and dipolar moment in the laboratory frame (*42*). These experiments pave the way for manipulating polar molecules in an optical lattice to form synthetic quantum materials, as discussed in the second part of this Review.

Products

Having prepared the reactants, it is necessary to observe and perhaps even control the products of reaction. This development, too, has a long history in beam experiments. The principal ambition of product investigation is to ascertain which chemical species emerge, in which internal states, and moving in which direction. The first two factors are often accessible by means of standard spectroscopic techniques, such as laser-induced fluorescence.

To measure the velocities of outgoing products, techniques such as velocity map imaging (VMI) are used (*43*). An outgoing molecule is first selectively ionized with little perturbation of its momentum. An electric field then guides the ion to a multichannel plate, which records the location of its arrival. The mass and charge of the ion and the shape of the electric field connect the original velocity of the molecule to the impact location on the plate.

To capitalize on the velocity distribution and extract the angular distribution of products requires that the velocities be referred to a well-defined incident axis of the collision. VMI techniques are thus most useful when the incident beams are as well controlled as possible, using techniques described above. This type of control was achieved, at least for inelastic scattering, by the van de Meerakker group, who crossed a pulsed beam with a Stark decelerator. This experiment succeeded in measuring narrow diffraction oscillations in the differential cross sections of NO scattering from rare-gas atoms (*44*).

In the coldest of samples, residing in traps, measurements of differential cross sections are problematic precisely because there is no well-defined initial direction for collisions, given that the molecules are traveling in many different directions. Still, identifying the products and their distribution into internal states can prove valuable. Many trapped-molecule experiments are not well suited to measuring products, at least at present. Part of the problem is that the products of reaction can emerge with large kinetic energies, on the order of electron volts (corresponding to many thousands of kelvins) and therefore are not themselves trapped for further study. At least two types of experiments can circumvent this issue, however.

The first of these was recently demonstrated by the Weinstein group, studying the reaction Li + CaH → LiH + Ca (*45*). This experiment was conducted not in a trap but in a helium buffer gas cell at a few kelvins, where both the reactants and products were stored. Despite releasing 0.9 eV of energy in the reaction, the products quickly cooled to the ambient temperature and were available for interrogation. Rotational levels cooled quickly, so their nascent distribution after reaction was undetermined. However, vibrational relaxation is notoriously slow in a buffer gas, meaning that vibrational populations produced from the reaction were still available for viewing.

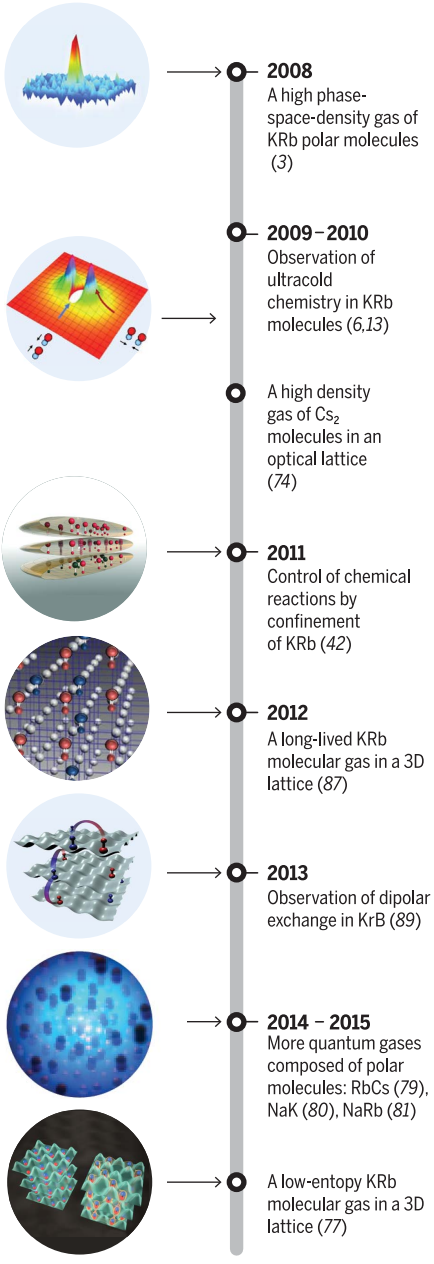

Fig. 3. Experimental progress since 2008 toward production of a quantum gas of bialkali molecules.

A second option for harnessing the products is provided by ion traps. Owing to the comparative strength of electromagnetic field confinement, molecular ions can be trapped even after they react, if the product is also electrically charged. Ions in such a trap arrange themselves into a "Coulomb crystal," where they can be individually observed by fluorescence. When a slowed reactant beam flows through the crystal, reactions can be observed one by one as the ions vanish from the crystal, providing the ultimate number resolution of a chemical reaction.

If the products happen also to be ionic, they can be sympathetically cooled by the original ions and join the Coulomb crystal themselves. This has occurred, for example, in the experiments of the Softley group (*46*), where certain calcium ions would disappear from the crystal during the reaction $Ca^+ + CH_3F \rightarrow CaF^+ + CH_3$. The CaF^+ ions were also trapped and made their presence known by perturbing the Ca^+ crystal, even though CaF^+ was not directly observed. Knowing it is there, though, makes it ripe for exploration.

Transition states

Careful preparation of reactants and observation of products often yield no progress toward the even greater challenge of observing or manipulating intermediates during the reaction. Generally, following the reaction in transition is the job of theory. However, the reaction itself contains useful handles by which it can be manipulated. These handles appear in the form of resonant states or transition states of the collision complex. That is to say, if reactants A and B (each of which may consist of many atoms) collide, they may form various configurations of all the atoms in the AB cluster, before finding their way to the products of reaction. This situation can lead to a resonant enhancement of the cross section at the energy of the AB cluster.

One such set of cluster states constitutes the van der Waals states, where clusters are held together by the weakly attractive van der Waals interaction between molecules but prevented initially from reacting by an energetic barrier (*47*). More intricate resonant states, termed transition state resonances, may exist behind the barrier. Observing and characterizing these resonances can shed light on the way in which the atoms share energy and pass it between them, giving hints about the chemical process. Cold, controlled collisions of reactants may allow the energy resolution necessary to observe these resonances. Moreover, if the resonant states happen to have magnetic or electric moments different from those of the reactants, then it is possible to apply a corresponding field to scan one or more resonances through the collision energy. This is a process long known and extremely useful in

ultracold scattering of atoms (*48*). For chemistry, its power is only starting to be appreciated—for example, in recent detailed calculations of H + LiF → Li + HF reactions by Tscherbul and Krems, who predict tremendous variation of rotational product states when driving electric field resonances in this system (*49*).

Another recent, striking example shows the interplay of theory and experiment in such cases. This study involved collisions of H_2 molecules with excited (metastable) helium atoms, leading to an ionization process whose products were easily detected (*50*). The potential energy surface that dictates this reaction is dependent on the angle θ between the axis of H_2 and the line joining the center of mass of H_2 to the He atom, as well as the distance R between the atom and the molecule.

This angular dependence was probed resonantly in the experiment, as follows. The potential energy V is generally written as an expansion into Legendre polynomials P, $V(R, \theta) = V_0(R)P_0(\cos\theta) + V_2(R)P_2(\cos\theta)$. If the molecule was prepared in a rotationless quantum state, with rotation quantum number $j = 0$, then the collision could not experience the anisotropy afforded by P_2, and a featureless cross section resulted from scattering owing to the isotropic component V_0. However, preparing the molecule in a $j = 1$ state effectively allowed the collision to probe the complete potential, including anisotropy and a resonant state (Fig. 2, bottom). The determination of the resonant energy places a tight constraint on the calculations of the potential energy surface. As pointed out by Simbotin and Côté, because of molecular symmetry, preparing the H_2 molecule in $j = 0$ or $j = 1$ is a matter of selecting its spin state (*51*). Thus, this reaction is another case in which reactions taking place at electron volt energies are controlled by nuclear spin degrees of freedom associated with a much smaller energy scale.

Finding resonances in scattering can thus be informative, but serious theory is needed to render interpretation useful. This is not a drawback, because the ultimate goal is interpretation. Still, as an alternative, direct spectroscopic probes of transition states are desirable. The power of spectroscopy was demonstrated, for example, in the benchmark chemical reaction F + H_2 → HF + H (*52*). In this case, the experiment began with ground-state clusters of all three atoms, with an electron attached. From these FH_2^- clusters, the electron was easily detached by light absorption, yielding resonances that could be attributed to transition states of the neutral FH_2 complex. As a result, it was possible to study the energetics and identity of the transition states.

After capturing the transition states, the ensuing goal is to understand the dynamics that drive the atoms through them, from reactants to products. Such a task would seem to require the spectroscopic accuracy of measuring the transition states, coupled with the time resolution to determine their populations in real time. In recent years, such a tool, with broad spectroscopic capabilities and very fine time resolution, has indeed been developed in the form of infrared frequency comb spectroscopy (*53*).

The power of this tool was unleashed very recently, in the atmospherically important reaction OH + CO → H + CO_2 (*54*). This reaction is known to proceed by forming a transition state HOCO, in both the trans and cis forms, which must surmount an energetic barrier before it can proceed to the products. While flopping around in this transition state, the complex can be affected in one of two ways by collisions with molecules in its environment. These collisions can either relax the complex into a lower energy state, stifling the reaction, or else activate it to higher energies, promoting its passage across the barrier. Watching the population of the state as a function of time revealed the relative rates of successful and unsuccessful reactions as a function of the background pressure.

An important challenge associated with the pursuit of full quantum control over molecular processes is the breadth of a technique's applicability with respect to the full menagerie of interesting molecular species. Whereas some techniques, such as laser cooling, do require very specific optical sources for each molecule, many techniques successfully maintain much greater generality, including buffer gas cooling, molecular decelerators, and frequency comb spectroscopy.

Theory and prospects

Amid the slew of experimental developments bringing new and detailed information on chemical reaction dynamics, the role of theory remains central to the ultimate goals of interpretation. The basic theoretical tools—construction of potential energy surfaces and scattering calculations based on those surfaces—are well established, as detailed in a vast literature. A survey in the context of cold molecules is provided by (*7*).

These calculations evolve in tandem with experimental data of ever-increasing quality, aided by increasing computational technology, but also by insights emerging from theoretical study. As an example of the latter, Cui and Krems have recently explored information-theoretic approaches to extract complex potential energy surfaces from a limited set of calculations (*55*). Insights such as these can substantially reduce the computational effort required to gain understanding.

In the longer term, a vast array of experimental and theoretical avenues is closing in on the ultimate expression of what chemical reactions can reveal. Consider that in the end, quantum mechanics imposes discreteness on everything:

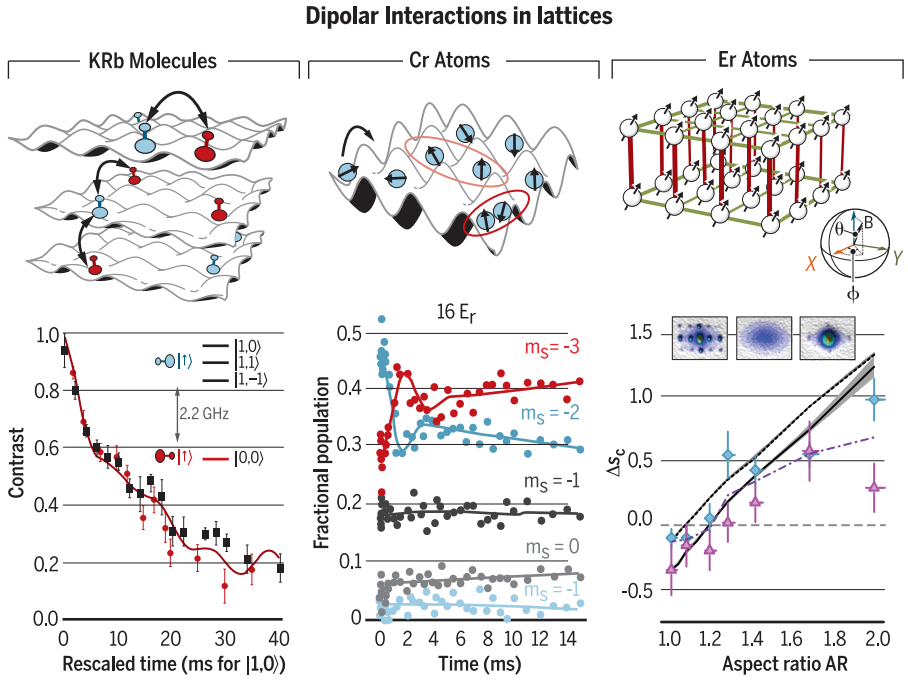

Fig. 4. Experimental observation of dipolar interactions in 3D lattices, using polar molecules and magnetic atoms. (**Left**) Measurement of Ramsey fringe contrast in a sparsely filled and deeply confining 3D lattice of KRb molecules with spins encoded in the two rotational states (*89*). (**Middle**) Measurement of the fractional Zeeman population in a bosonic Cr gas in a lattice. Here, $|m_s| = 0, 1, 2$, and 3 label the different Zeeman levels. The case shown corresponds to a lattice depth of $16E_r$ (E_r is the photon recoil energy), where tunneling is largely suppressed and the spin dynamics are mainly induced by dipolar exchange processes between neighboring sites. [Adapted from (*93*, *94*) with permission and copyrighted by the American Physical Society] (**Right**) Modification of the critical lattice depth of the superfluid-to-Mott insulator transition as a result of the magnetic dipolar interaction between spin-polarized Er atoms. The dipolar interaction modifies the lattice depth at which the phase transition takes place in a way that depends on the atomic cloud geometry and dipole orientation. Δs_C is the difference in the critical value of the lattice depth for two different dipole orientations, $\theta = 0°$ and $\theta = 90°$. The angle was varied by changing the direction of the polarizing magnetic field. [Adapted from (*95*) with permission]

GRAPHIC: ADAPTED BY N. CARY/*SCIENCE*

Molecules have well-defined states in all internal degrees of freedom, from electronic structure all the way down to nuclear spin. Moreover, in the ultracold limit, even the relative motion of the reactant molecules becomes quantized into discrete partial waves, as was exploited in the KRb experiment discussed above.

Therefore, considering α to stand for the collection of quantum numbers of all reactant states, and β to stand for that of all product states, the prospect of constructing the entire scattering matrix $S_{\alpha\beta}$ can be envisioned. This would constitute the "complete chemical experiment," whose analog in inelastic electron-atom or atom-atom scattering has been contemplated for decades (*56*). Chemistry affords the opportunity to go even beyond this, when reaction intermediates and transition states are also observed. This activity would require the most stringent cooperation of experiment and theory and would presumably teach us the most that nature permits us to know about a given reaction.

Quantum materials

The realization of atomic Bose-Einstein condensation (BEC) set the stage for the creation of a new form of materials, synthesized quantum matter, that has stimulated insights into the development of many-body quantum correlations and fostered intimate connections between atomic, molecular, and optical (AMO) and condensed matter physics (*57*). The capability of experimental control in nearly all possible aspects of atomic quantum gases facilitated the studies of BEC properties out of equilibrium, such as the dynamics of vortices and solitons (*58*). The production of atomic degenerate Fermi gases (*59*) opened a window to the exploration of outstanding scientific questions in areas such as superconductivity and superfluidity (*60*, *61*), as well as tabletop studies of strongly correlated quantum fluids analogous to those formed in neutron stars and nuclear matter under strong interactions. In parallel, optical lattices, where atoms are loaded in an artificial periodic potential generated by laser light, have allowed the realization of simplified crystals with highly tunable geometry, degree of disorder, and strength of interactions. This development has led to many groundbreaking observations (*62*), such as the transition from a weakly interacting fermionic or bosonic gas to a Mott insulator, a strongly correlated state where the large interatomic interactions prevent atomic motion and favor the formation of a structure with a fixed number of atoms per lattice site.

Building on these successes, to further advance our understanding of complex quantum materials and provide insights into dynamical processes arising from strong correlations, important obstacles need to be overcome in this field. In fact, many key phenomena of crucial importance in condensed matter physics remain difficult to achieve and probe in state-of-the-art cold atom experiments. Take the example of quantum magnetism, the fundamental origin of which has many open questions. Magnetic behavior in electronic materials emerges as a consequence of intricate interplays between quantum statistics, spin-orbit coupling, and motional effects, as well as electromagnetic interactions. Magnetic correlations are often believed to be closely connected with unconventional superconductivity (*63*–*65*) and are at the heart of a large class of topological states of matter that are beyond the conventional description of the "Landau paradigm" of symmetry breaking (*66*). Generating nonlocal spin-spin interactions in a generic cold atom system is challenging because their contact interaction is short-ranged and magnetic dipole interactions are weak. When mediated with motion, magnetic correlations emerge only when the motional energy is less than the effective spin-spin coupling energy. Polar molecules, on the other hand, possess strong and long-range interactions with an enlarged set of internal states that offer a more versatile platform for building synthetic quantum matter (*9*, *10*, *38*–*40*, *67*–*70*). The basic question, then, is whether one can develop a quantum system of molecules that features precise quantum control at the same level as that demonstrated in atomic quantum gas experiments. Whereas the frontier of cold molecules has been fairly broad—using a diverse set of experimental approaches, as discussed in the first part of this Review—the path toward the production of a quantum gas of polar molecules has been substantially more focused. In the remainder of this Review, we will describe the only successful approach so far, which is based on bialkali polar molecules.

There are other AMO systems under experimental investigation, including trapped ions (*71*), Rydberg atoms (*72*, *73*), and magnetic atoms (*70*), and they all offer the prospect of long-range interactions and a set of alternative attributes. In this survey, however, we focus on polar molecules.

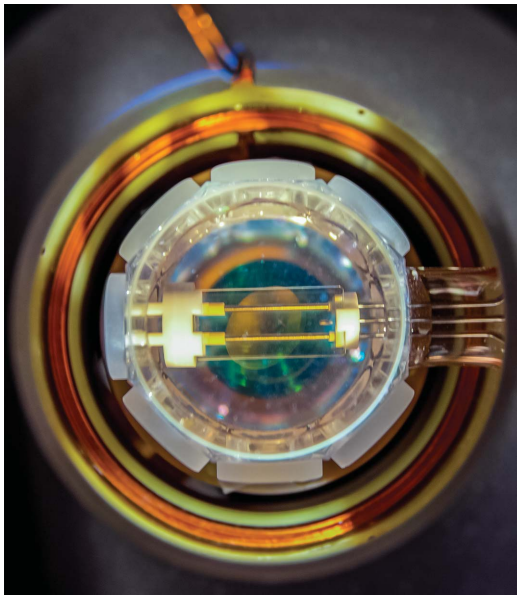

The transparent electrodes used to manipulate polar KRb molecules confined by an optical lattice inside an ultrahigh vacuum cell.

PHOTO: L. DE MARCO

Quantum degeneracy of a molecular gas

Polar diatomic molecules are excellent candidates for the investigation of magnetic phenomena. On the one hand, they possess a permanent dipole moment that can be manipulated with external fields and that provides long-range anisotropic dipolar interactions. On the other hand, they exhibit a hierarchy of internal degrees of freedom, including hyperfine, rotational, vibrational, and electronic levels. Once controlled, the intricate internal structure provides a high degree of flexibility and specificity to engineer a quantum system by using external fields to couple molecules directly through dipolar interactions, without the need of motional processes. A fundamental requirement to take full advantage of these attributes is the capability to prepare a molecular quantum gas.

As discussed in the first part of this Review, cooling molecular gases to the quantum regime is extremely challenging. In fact, none of the techniques discussed so far for direct cooling of molecules have come close to the quantum degenerate regime: Most have produced molecular PSDs that are about 10 to 12 orders of magnitude lower than those required for quantum degeneracy.

In 2008, a revolutionary path emerged for successful production of an ultracold polar molecular gas near quantum degeneracy (Fig. 3). In this approach, ultracold polar molecules were coherently assembled from two atomic species that had themselves been brought to quantum degeneracy. Specifically, the Jin and Ye groups used a Fano-Feshbach resonance (*48*) for magneto-association of pairs of fermionic ^{40}K and bosonic ^{87}Rb atoms (*3*). These weakly bound (highly vibrationally excited) Feshbach molecules were then coherently transferred to the absolute rovibrational ground state in the ground electronic potential by using a pair of phase-coherent lasers coupled to a common intermediate electronic excited state. This population transfer process, known as stimulated Raman adiabatic passage (STIRAP), is fully coherent in that nearly 100% of the Feshbach molecules were transferred to the single ground state while imparting hardly any heating to the molecular gas. [STIRAP was also used by the Nägerl group to create ground-state homonuclear Cs_2 molecules (*74*).] Once in the rotational-vibrational-electronic ground state, molecules were transferred to the hyperfine ground level by using microwave fields that coupled the ground and first excited rotation states (*75*, *76*). The net result was a gas of fermionic ^{40}K^{87}Rb molecules at its lowest internal energy state with a temperature of ~100 nK and a PSD just around the onset of quantum degeneracy. Expressed in terms of the Fermi temperature (T_F), the temperature of the molecular gas was about $T/T_F \approx 1.5$. Further improvements in this method have recently led to the production of a quantum gas of ^{40}K^{87}Rb loaded in a 3D optical lattice, with entropy of $2.2k_B$ per molecule,

corresponding to that of a bulk Fermi gas with $T/T_F \approx 0.3$ (*77*).

In recent years (Fig. 3), the production of rovibrational ground-state molecules has also been achieved for several other bialkali species, such as Cs_2 (*74*), RbCs (*78*, *79*), NaK (*80*), and NaRb (*81*). This effort is motivated partly by the desire to avoid the exothermic reaction as experienced by KRb molecules (*82*), and partly by the appeal of larger dipole moments (*83*). However, it is possible to have molecular loss through a three-body collision process, during which two molecules collide and temporarily form a reaction complex when a third molecule approaches sufficiently closely, which forces inelastic loss of all three molecules (*84*). With a number of research groups worldwide actively working on polar molecular quantum gas experiments, we can expect that some of these open questions will be addressed and that a diverse set of quantum gases of polar molecules will become available in the near future.

Dealing with reactive losses

Although the original motivation of the KRb experiment for the creation of a molecular quantum gas was to study correlated quantum matter, the experiment turned into an opportunity to study chemical reactions near absolute zero, where simple quantum mechanical rules govern how single-state–controlled reactants approach each other. The two-body loss evident from a gas of ground-state KRb molecules confined in an optical dipole trap was attributed to an exothermic reaction process of KRb + KRb → K_2 + Rb_2, leaving the products with sufficiently high kinetic energies to almost instantaneously escape the optical trap (*6*, *13*). For the lowest collision partial wave (l = 1), the associated centrifugal barrier of 24 μK was considerably higher than the collision energy of ~100 nK. Thus, the reaction was largely suppressed, leading to a lifetime of ~1 s for a molecular density of 10^{12} cm^{-3} in the trap.

When an electric field is applied, molecules become oriented and exhibit a dipole moment in the laboratory frame. Dipolar interactions mix different partial wave collision channels, substantially altering the two-body collision process (*13*, *42*). In fact, the relevant quantum number to use is the projection of the angular momentum along the external field: When two molecules collide in a plane perpendicular to their oriented dipoles, the collisional energy barrier is increased; when they collide along their orientation axis, the barrier is lowered. For this reason, when both "side-to-side" and "head-to-tail" collisions were allowed under an applied electric field, the observed lifetime was reduced to a few milliseconds at typical molecular densities of 10^{12} cm^{-3} in the trap (Fig. 3).

The control of dipole-mediated chemical reactions was demonstrated by suppressing the undesirable "head-to-tail" collisions by means of tight confinement in geometries that only energetically allow repulsive interactions. For example, by trapping molecules in an array of quasi-2D disks generated by interfering an optical beam (in the so-called 1D optical lattice) and aligning the dipoles by an external electric field perpendicular to the disks, chemical reactions were observed to slow down with increasing dipole moment (*42*, *85*, *86*). This experiment illustrates the use of optical lattices and electric field manipulation to render the molecules more stable for condensed matter purposes.

A tightly confining 3D optical lattice freezes out molecular motion in all directions (Fig. 3). Trapped in individual lattice sites, each molecule shows a lifetime longer than 20 s, limited only by off-resonant light scattering from the trapping beams (*87*). The strong intermolecular interactions, both reactive and conservative, guarantee that only one molecule can occupy a particular lattice site. Another intriguing quantum phenomenon manifests in the overall reaction rate of the molecular gas, the so-called quantum Zeno effect. The molecular loss rate is increasingly suppressed with an enhanced onsite reaction rate as a result of the tightened spatial confinement (*88*, *89*). When the onsite reaction rate far exceeds the tunneling rate, hopping of molecules between neighboring sites becomes a second-order process that is increasingly suppressed.

Synthetic quantum magnets

The preparation of a stable, low-entropy gas of polar molecules pinned in a 3D lattice set the stage for exploration of quantum magnetism mediated by dipolar interactions (Fig. 3). The word "magnetism" in this case refers to the modeling of an array of coupled spin-½ magnetic moments with an interacting spin-½ system where couplings are mediated by electric dipolar interactions (*38*–*40*): If a molecule located at site i with a dipole moment $\hat{\mathbf{d}}_i$ interacts via a dipolar interaction with another molecule at site j with a dipole moment $\hat{\mathbf{d}}_j$, the interaction is given by

$$\hat{H}_{ij}^{dd} = \frac{1}{4\pi\varepsilon_0}\left[\frac{\hat{\mathbf{d}}_i \cdot \hat{\mathbf{d}}_j - 3(\hat{\mathbf{r}}_{ij} \cdot \hat{\mathbf{d}}_i)(\hat{\mathbf{r}}_{ij} \cdot \hat{\mathbf{d}}_j)}{|\mathbf{r}_i - \mathbf{r}_j|^3}\right] \quad (1)$$

where $\mathbf{r}_{i,j}$ are the vectors describing molecular positions i and j, and $\hat{\mathbf{r}}_{ij} = \frac{\mathbf{r}_i - \mathbf{r}_j}{|\mathbf{r}_i - \mathbf{r}_j|}$ is the unit vector joining the molecules. If the molecules are prepared and controlled to populate only two opposite-parity rotational states, denoted as $|\uparrow\rangle$ and $|\downarrow\rangle$, then the dipole-dipole interaction Hamiltonian can be expressed in terms of spin-½ angular momentum operators ($\hat{S}$) acting on the (↑, ↓) states. The resulting Hamiltonian, $\hat{H}^S$, represents an XXZ spin-½ system, which is an iconic model for quantum magnetism

$$\hat{H}^S = \sum\nolimits_{ij} \hat{H}_{ij}^S$$

$$\hat{H}_{ij}^S = V_{dd}(\mathbf{r}_i - \mathbf{r}_j)[J^{\perp}(\hat{S}_i^+\hat{S}_j^- + \hat{S}_i^-\hat{S}_j^+) + J^Z\hat{S}_i^Z\hat{S}_j^Z + W(\hat{S}_i^Z + \hat{S}_j^Z)] \quad (2)$$

where $V_{dd}(\boldsymbol{r}_i - \boldsymbol{r}_j) = [1 - 3\cos^2(\Theta_{ij})]/|\boldsymbol{r}_i - \boldsymbol{r}_j|^3$, and Θ_{ij} is the angle between the quantization axis (set by the external electromagnetic field) and $\hat{\mathbf{r}}_{ij}$. The long-range and anisotropic coupling constants are fully determined by the off-diagonal ($J^{\perp}$) and diagonal (J^Z and W) dipole matrix elements and can be tuned through the strength of the external field or the choice of the rotational state. Whereas J^Z (Ising interaction) and W vanish under zero electric field, $J^{\perp}$ (exchange interaction) remains finite and is intrinsically related to the transition dipole moment between the chosen pair of rotational states, $\langle\uparrow|\hat{\mathbf{d}}|\downarrow\rangle$.

The first experimental implementation of $\hat{H}^S$ was realized in 2013 (*89*), using a 3D optical lattice sparsely filled with 10^4 KRb molecules (~5%). The molecules were initially prepared in the rovibrational ground state $|\downarrow\rangle = |N = 0, m_N = 0\rangle$, where N is the principal rotational quantum number and m_N is its projection onto the quantization axis set by an external magnetic field. The hyperfine interaction lifts the degeneracy of the N = 1 rotational manifold; consequently, either $|N = 1, m_N = -1\rangle$ or $|N = 1, m_N = 0\rangle$ could be selected as $|\uparrow\rangle$ by a microwave field to couple with $|\downarrow\rangle$. Under a zero dc electric field, only the $J^{\perp}$ term contributes to the dynamics by flipping spins between pairs of molecules in opposite spin configuration, $|\uparrow\downarrow\rangle \leftrightarrow |\downarrow\uparrow\rangle$. After preparing a 50-50 coherent superposition, the system was allowed to freely evolve under $\hat{H}^S$ for some time, after which the collective spin coherence was probed with the application of a second microwave π/2 pulse, followed with a spin population readout.

Of course, precise control of single-molecule quantum states played an important role in the study of many-body physics. The real part of the molecular polarizability gives rise to the ac Stark shift that helps trap molecules in the lattice. The polarizability can be precisely controlled by varying the angle between the polarization of the lattice light and the quantization field defined by an applied electric or magnetic field. At a specific angle, the polarizability of the two rotational states used as $|\uparrow\rangle$ and $|\downarrow\rangle$ becomes equal, thus minimizing the differential ac Stark shift between the two spin states, leading to prolonged spin coherence times (*90*). A coherence time of ~1 s was recently achieved between two hyperfine states of NaK in its ground rotational state (*91*).

The molecular spin-½ Hamiltonian resulted in clear experimental signatures for interacting many-body dynamics mediated by dipolar exchange interaction. The spin evolution fringe shown in Fig. 4, left, includes small-amplitude oscillations at the frequencies determined by the exchange rate of rotational excitations between pairs of nearest-neighbor and next-to-nearest-neighbor molecules. The existence of several oscillation frequencies, arising from interactions of molecules separated by a few discrete distances in the lattice, results in an overall exponential decay of the fringe signal with a rate that is proportional to the lattice-filling fraction. A specific dynamical decoupling pulse sequence can be designed to disentangle pairs of molecules under spin exchange and thus suppress the oscillation. All of these experimental observations

have been supported by numerical calculations based on the $\hat{H}^S$ Hamiltonian (*92*).

Similar types of exchange processes have been observed using bosonic ^{52}Cr atoms prepared in a Mott insulator state in a 3D lattice (*93*, *94*). In those experiments, the spin was encoded in hyperfine states of the atoms and coupled by magnetic dipolar interactions. In the deep lattice limit when motion is frozen, the dynamics are described with a similar XXZ model. In contrast to the spin-½ KRb experiment, each Cr atom encodes a spin-3. For this system, the average populations for different spin sublevels and the total gas magnetization are not locked, and therefore the spin-exchange dynamics can manifest directly in the spin population, without spin coherence, as was the case for KRb (Fig. 4, middle). Although magnetic interactions are generically weaker than electric dipolar interactions, the use of a smaller lattice constant under a higher filling fraction enabled the observation of the magnetically induced spin-exchange dynamics in the ^{52}Cr experiment. Moreover, the experiment revealed the interplay between tunneling, onsite contact interactions, and dipolar exchange magnetism (*93*).

This interplay has also been observed in a recent experiment with spin-polarized ^{168}Er atoms in a 3D lattice (*95*) (Fig. 4, right). The long-range and anisotropic magnetic dipolar interactions introduced substantive modifications to the superfluid-to-Mott insulator transition. For example, the critical point of the phase transition was observed to depend on the magnetic field direction and the aspect ratio of the trapped Er atomic gas.

Recently, another important step toward the creation of a low-entropy gas of polar molecules in a lattice was accomplished through the development of a quantum synthesis protocol (Fig. 3) (*77*, *96*). The idea was to create dual atomic insulators—a Rb Mott insulator and a K band insulator—in the same optical lattice, to maximize the number of individual lattice sites populated with exactly one atom from each species. This experiment required solving a number of challenges arising from the opposing requirements of the Bose and Fermi statistics associated with the two species, as well as their distinct masses and polarizabilities and the need to control the interspecies interactions during the state preparation and the magneto-association process. The protocol yielded a filling fraction of >25% of ground-state KRb molecules in the 3D lattice (*77*), corresponding to an entropy per molecule of just $2k_B$. In this situation, the filling has reached the percolation threshold, where no isolated patch of molecules may exist in the lattice without feeling interactions that are sufficiently strong for correlations with the rest of the system. A variant of this protocol was recently used to produce low-entropy samples of RbCs Feshbach molecules (*97*). Future experimental improvements based on this work should be able to increase the filling further to 50% (*98*).

Future prospects: Advanced materials

The successful observation of dipole-induced quantum magnetism even in a sparsely filled molecular lattice points to a broad arena of exciting physics waiting to be explored. Reaching higher lattice fillings, improving imaging resolution, and implementing stronger electromagnetic field control of the coupling constants will most likely make this strongly correlated quantum system computationally inaccessible with classical technologies. This quantum simulator could allow exploration of complex, nonequilibrium spin dynamics and tracking of the propagation of quantum correlation, thermalization, and buildup of entanglement in long-range interacting spin systems (Fig. 5, bottom) (*99*). This would constitute the first experimental system where the spatial dimensionality and the scaling of the range of interactions with respect to the interparticle distance are the same—making it a unique benchmarking system in an area that, so far, is intractable to theory. Moreover, empty sites in the lattice could be used as defects; hence, this platform could be used for studies of spin transport and many-body localization (MBL) by tuning the molecular filling and dipolar interaction strength (*100*). A system displaying MBL transports neither heat nor charge (where by "charge," we mean mass), even when the amount of energy injected is macroscopic. MBL is of great interest, in part because a system displaying it may be used as a robust quantum memory or for implementation of topological order.

The thermodynamic phase diagram of $\hat{H}^S$ featuring effective long-range and anisotropic interactions is not realizable with existing classical computers. This type of model falls under the class of strongly frustrated systems, where competing interactions can prevent classical ordering even at zero temperature, exhibiting a magnetic analog of liquid phases (*101*). Such quantum spin liquids are highly entangled and can show nontrivial topological behavior similar to that found in the fractional quantum Hall effect, including fractionalized excitations and robust chiral edge modes. The elucidation of phase transitions and diagrams by means of ultracold molecules would be a major advance in our understanding of strongly interacting systems (*102*).

Involving a larger set of rotational states in molecules would enable exploration of the emergence of spin-orbit coupling (SOC) in pinned dipoles (Fig. 5, middle). SOC in solids is a key to understanding a variety of spin-transport and topological phenomena, such as Majorana fermions and recently discovered topological insulators. Implementing and controlling SOC in a synthetic quantum material is thus highly desirable. Despite major advances in using alkali metal atoms to realize SOC (*103*–*105*), such implementations have been hindered by heating from spontaneous emission, which has limited the observation of many-body effects. For polar molecules, SOC can naturally emerge without the need for external laser fields because it is a result of dipolar interaction–induced transfer of angular momentum between the internal rotational states. It manifests as spin excitations that carry a nonzero Berry phase. Recent theoretical studies have found that, depending on the number of degenerated rotational states and the geometry of the molecular lattice, the excitations can exhibit band structures similar to chiral excitations in bilayer graphene (*106*) or to Weyl quasiparticles (*107*). Experimental observables would include the density profile, spin currents, and spin coherences.

Dressing of molecules with microwave or optical fields leads to a rich landscape of possibilities when multiple rotational states are involved. This enables the design of models in which the strength of the spin couplings depends on the spatial direction, which is predicted to lead to symmetry-protected topological phases (*108*, *109*) or phases with true topological order, such as fractional Chern insulators (*110*, *111*).

The next phase of research may target several additional features of magnetism in real materials (Fig. 5, top). For example, magnetic interactions in real materials result from a complex variety of mechanisms, including exchange, superexchange,

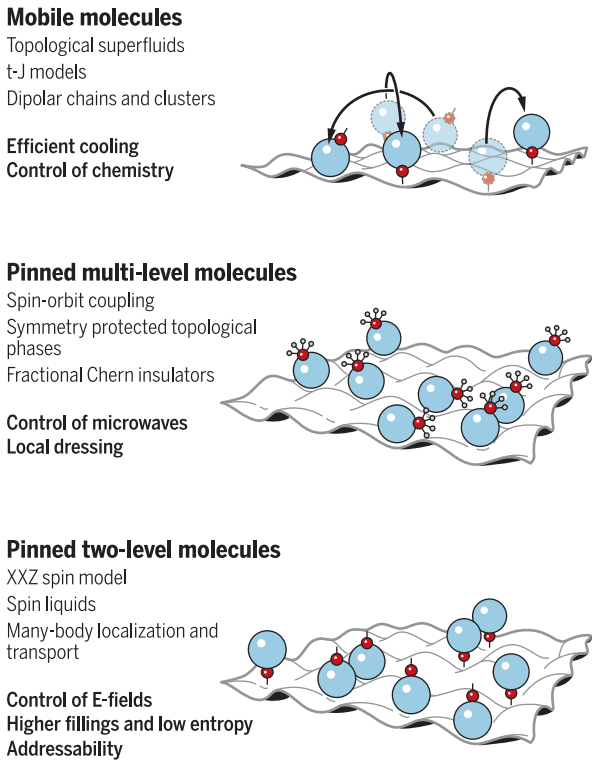

Fig. 5. A range of prospective advanced quantum materials assembled with ultracold molecules.

and itinerant particles, occurring both in combination and in competition. An iconic example is the so-called *t-J* model (*112*), which is believed to contain the essential ingredients (tunneling, density-density interactions, and spin-spin interactions) to describe the high-temperature superconducting state that emerges when a Mott insulator is doped. Although deceivingly trivial in mathematical expression, the model contains complex physics and is intractable with classical methodologies. If the temperature of a molecular quantum gas is lowered further, and the chemical reaction is controlled at the desired level, then the exchange interactions in the long-range analog of the *t-J* model will manifest rich dynamics in a dipolar gas (*113*).

Reaching a higher PSD required for the observation of itinerant magnetism might be possible by evaporatively cooling the molecular quantum gas. This requires tight confinement of the molecular gas into quasi-2D traps, stable under a strong dc electric field (*85*). Most of the necessary capabilities for this are under experimental development. For molecules prepared in the same internal state in a stack of 2D traps, an intriguing prospect that evaporative cooling will open is the formation of dipolar chains and clusters extending over multiple trap sites (*67*, *68*, *70*). Such structures are stabilized by the intralayer attraction. In the presence of appropriate microwave dressing, intralayer dipolar attraction can also stabilize a $p_x + ip_y$ topological superfluid, a target for topologically protected quantum information processing (*68*).

REFERENCES AND NOTES

1. G. Scoles, D. Bassi, U. Buck, Eds., *Atomic and Molecular Beam Methods*, vol. 1 (Oxford Univ. Press, 1988).
2. M. Shapiro, P. Brumer, *Quantum Control of Molecular Processes* (John Wiley & Sons, 2012).
3. K. K. Ni *et al*., *Science* **322**, 231–235 (2008).
4. A. Teslja, J. J. Valentini, *J. Chem. Phys.* **125**, 132304 (2006).
5. R. D. Levine, *Molecular Reaction Dynamics* (Cambridge Univ. Press, 2005).
6. S. Ospelkaus *et al*., *Science* **327**, 853–857 (2010).
7. N. Balakrishnan, *J. Chem. Phys.* **145**, 150901 (2016).
8. G. Quéméner, P. S. Julienne, *Chem. Rev.* **112**, 4949–5011 (2012).
9. L. D. Carr, D. DeMille, R. V. Krems, J. Ye, *New J. Phys.* **11**, 055049 (2009).
10. M. Lemeshko, R. V. Krems, J. M. Doyle, S. Kais, *Mol. Phys.* **111**, 1648–1682 (2013).
11. R. V. Krems, W. C. Stwalley, B. Friedrich, Eds., *Cold Molecules: Theory, Experiment, Applications* (CRC Press, 2009).
12. N. Balakrishnan, A. Dalgarno, *Chem. Phys. Lett.* **341**, 652–656 (2001).
13. K. K. Ni *et al*., *Nature* **464**, 1324–1328 (2010).
14. N. Mukherjee, R. N. Zare, *J. Chem. Phys.* **135**, 024201 (2011).
15. A. B. Henson, S. Gersten, Y. Shagam, J. Narevicius, E. Narevicius, *Science* **338**, 234–238 (2012).
16. N. R. Hutzler, H. I. Lu, J. M. Doyle, *Chem. Rev.* **112**, 4803–4827 (2012).
17. S. Y. T. van de Meerakker, H. L. Bethlem, G. Meijer, *Nat. Phys.* **4**, 595–602 (2008).
18. J. J. Gilijamse, S. Hoekstra, S. Y. T. van de Meerakker, G. C. Groenenboom, G. Meijer, *Science* **313**, 1617–1620 (2006).
19. M. I. Fabrikant *et al*., *Phys. Rev. A* **90**, 033418 (2014).
20. S. Hoekstra *et al*., *Phys. Rev. A* **76**, 063408 (2007).
21. B. C. Sawyer *et al*., *Phys. Rev. Lett.* **98**, 253002 (2007).
22. T. Rieger, T. Junglen, S. A. Rangwala, P. W. H. Pinkse, G. Rempe, *Phys. Rev. Lett.* **95**, 173002 (2005).
23. B. C. Sawyer, B. K. Stuhl, D. Wang, M. Yeo, J. Ye, *Phys. Rev. Lett.* **101**, 203203 (2008).
24. B. C. Sawyer *et al*., *Phys. Chem. Chem. Phys.* **13**, 19059–19066 (2011).
25. A. Prehn, M. Ibrügger, R. Glöckner, G. Rempe, M. Zeppenfeld, *Phys. Rev. Lett.* **116**, 063005 (2016).
26. B. K. Stuhl *et al*., *Nature* **492**, 396–400 (2012).
27. D. Reens, H. Wu, T. Langen, J. Ye, Molecular spin-flip loss and a dual quadrupole trap. arXiv:1706.02806 [physics.atom-ph] (9 June 2017).
28. M. D. Di Rosa, *Eur. Phys. J. D* **31**, 395 (2004).
29. B. K. Stuhl, B. C. Sawyer, D. Wang, J. Ye, *Phys. Rev. Lett.* **101**, 243002 (2008).
30. E. S. Shuman, J. F. Barry, D. Demille, *Nature* **467**, 820–823 (2010).
31. M. T. Hummon *et al*., *Phys. Rev. Lett.* **110**, 143001 (2013).
32. J. F. Barry, D. J. McCarron, E. B. Norrgard, M. H. Steinecker, D. DeMille, *Nature* **512**, 286–289 (2014).
33. B. Hemmerling *et al*., *J. Phys. At. Mol. Opt. Phys.* **49**, 174001 (2016).
34. J. A. Devlin, M. R. Tarbutt, *New J. Phys.* **18**, 123017 (2016).
35. L. Anderegg *et al.,* Radio frequency magneto-optical trapping of CaF with high density. arXiv:1705.10288 [physics.atom-ph] (29 May 2017).
36. S. Truppe *et al.,* Molecules cooled below the Doppler limit. arXiv:1703.00580 [physics.atom-ph] (2 March 2017).
37. L. M. C. Janssen, G. C. Groenenboom, A. van der Avoird, P. S. Zuchowski, R. Podeszwa, *J. Chem. Phys.* **131**, 224314 (2009).
38. B. Gadway, B. Yan, *J. Phys. At. Mol. Opt. Phys.* **49**, 152002 (2016).
39. S. A. Moses, J. P. Covey, M. T. Miecnikowski, D. S. Jin, J. Ye, *Nat. Phys.* **13**, 13–20 (2017).
40. M. L. Wall, K. R. A. Hazzard, A. M. Rey, in *From Atomic to Mesoscale*, S. A. Malinovskaya, I. Novikova, Eds. (World Scientific, 2014), pp. 3–37.
41. A. Micheli, G. Pupillo, H. P. Buchler, P. Zoller, *Phys. Rev. A* **76**, 043604 (2007).
42. M. H. G. de Miranda *et al*., *Nat. Phys.* **7**, 502–507 (2011).
43. J. J. Lin, J. G. Zhou, W. C. Shiu, K. P. Liu, *Rev. Sci. Instrum.* **74**, 2495–2500 (2003).
44. A. von Zastrow *et al*., *Nat. Chem.* **6**, 216–221 (2014).
45. V. Singh *et al*., *Phys. Rev. Lett.* **108**, 203201 (2012).
46. S. Willitsch, M. T. Bell, A. D. Gingell, S. R. Procter, T. P. Softley, *Phys. Rev. Lett.* **100**, 043203 (2008).
47. N. Balakrishnan, *J. Chem. Phys.* **121**, 5563–5566 (2004).
48. C. Chin, R. Grimm, P. Julienne, E. Tiesinga, *Rev. Mod. Phys.* **82**, 1225–1286 (2010).
49. T. V. Tscherbul, R. V. Krems, *Phys. Rev. Lett.* **115**, 023201 (2015).
50. A. Klein *et al*., *Nat. Phys.* **13**, 35–38 (2017).
51. I. Simbotin, R. Cote, *New J. Phys.* **17**, 065003 (2015).
52. J. B. Kim *et al*., *Science* **349**, 510–513 (2015).
53. A. J. Fleisher *et al*., *J. Phys. Chem. Lett.* **5**, 2241–2246 (2014).
54. B. J. Bjork *et al*., *Science* **354**, 444–448 (2016).
55. J. Cui, R. V. Krems, *Phys. Rev. Lett.* **115**, 073202 (2015).
56. H. Kleinpoppen, B. Lohmann, A. N. Grum-Grzhimailo, *Perfect/Complete Scattering Experiments: Probing Quantum Mechanics on Atomic and Molecular Collisions and Coincidences* (Springer, 2013).
57. I. Bloch, J. Dalibard, W. Zwerger, *Rev. Mod. Phys.* **80**, 885–964 (2008).
58. F. Dalfovo, S. Giorgini, L. P. Pitaevskii, S. Stringari, *Rev. Mod. Phys.* **71**, 463–512 (1999).
59. B. DeMarco, D. S. Jin, *Science* **285**, 1703–1706 (1999).
60. M. Randeria, E. Taylor, *Annu. Rev. Condens. Matter Phys.* **5**, 209–232 (2014).
61. S. Giorgini, L. P. Pitaevskii, S. Stringari, *Rev. Mod. Phys.* **80**, 1215–1274 (2008).
62. I. Bloch, *Nat. Phys.* **1**, 23–30 (2005).
63. G. R. Stewart, *Rev. Mod. Phys.* **83**, 1589–1652 (2011).
64. P. A. Lee, N. Nagaosa, X.-G. Wen, *Rev. Mod. Phys.* **78**, 17–85 (2006).
65. X.-L. Qi, S.-C. Zhang, *Rev. Mod. Phys.* **83**, 1057–1110 (2011).
66. C.-K. Chiu, J. C. Y. Teo, A. P. Schnyder, S. Ryu, *Rev. Mod. Phys.* **88**, 035005 (2016).
67. M. A. Baranov, *Phys. Rep.* **464**, 71 (2008).
68. M. A. Baranov, M. Dalmonte, G. Pupillo, P. Zoller, *Chem. Rev.* **112**, 5012–5061 (2012).
69. G. Pupillo, A. Micheli, H. P. Buchler, P. Zoller, in *Cold Molecules: Theory, Experiment, Applications*, B. F. R. V. Krems, W. C. Stwalley, Eds. (CRC Press, 2009), pp. 421–469.
70. T. Lahaye, C. Menotti, L. Santos, M. Lewenstein, T. Pfau, *Rep. Prog. Phys.* **72**, 126401 (2009).
71. R. Blatt, C. F. Roos, *Nat. Phys.* **8**, 277–284 (2012).
72. R. Löw *et al*., *J. Phys. B At. Mol. Opt. Phys.* **45**, 113001 (2012).
73. H. Labuhn *et al*., *Nature* **534**, 667–670 (2016).
74. J. G. Danzl *et al*., *Nat. Phys.* **6**, 265–270 (2010).
75. S. Ospelkaus *et al*., *Phys. Rev. Lett.* **104**, 030402 (2010).
76. S. A. Will, J. W. Park, Z. Z. Yan, H. Loh, M. W. Zwierlein, *Phys. Rev. Lett.* **116**, 225306 (2016).
77. S. A. Moses *et al*., *Science* **350**, 659–662 (2015).
78. T. Takekoshi *et al*., *Phys. Rev. A* **85**, 032506 (2012).
79. P. K. Molony *et al*., *Phys. Rev. Lett.* **113**, 255301 (2014).
80. J. W. Park, S. A. Will, M. W. Zwierlein, *Phys. Rev. Lett.* **114**, 205302 (2015).
81. M. Guo *et al*., *Phys. Rev. Lett.* **116**, 205303 (2016).
82. P. S. Zuchowski, J. M. Hutson, *Phys. Rev. A* **81**, 060703 (2010).
83. J. N. Byrd, J. A. Montgomery, R. Cote, *Phys. Rev. A* **86**, 032711 (2012).
84. M. Mayle, G. Quemener, B. P. Ruzic, J. L. Bohn, *Phys. Rev. A* **87**, 012709 (2013).
85. A. Micheli *et al*., *Phys. Rev. Lett.* **105**, 073202 (2010).
86. G. Quéméner, J. L. Bohn, *Phys. Rev. A* **83**, 012705 (2011).
87. A. Chotia *et al*., *Phys. Rev. Lett.* **108**, 080405 (2012).
88. B. Zhu *et al*., *Phys. Rev. Lett.* **112**, 070404 (2014).
89. B. Yan *et al*., *Nature* **501**, 521–525 (2013).
90. B. Neyenhuis *et al*., *Phys. Rev. Lett.* **109**, 230403 (2012).
91. J. W. Park, Z. Y. Yan, H. Loh, S. A. Will, M. W. Zwierlein, Second-scale nuclear spin coherence time of trapped ultracold $^{23}Na^{40}K$ molecules. arXiv:1606.04184v1 [cond-mat.quant-gas] (14 June 2016).
92. K. R. A. Hazzard *et al*., *Phys. Rev. Lett.* **113**, 195302 (2014).
93. A. de Paz *et al*., *Phys. Rev. A* **93**, 021603 (2016).
94. A. de Paz *et al*., *Phys. Rev. Lett.* **111**, 185305 (2013).
95. S. Baier *et al*., *Science* **352**, 201–205 (2016).
96. A. Safavi-Naini, M. L. Wall, A. M. Rey, *Phys. Rev. A* **92**, 063416 (2015).
97. L. Reichsöllner, A. Schindewolf, T. Takekoshi, R. Grimm, H.-C. Nägerl, *Phys. Rev. Lett.* **118**, 073201 (2017).
98. J. P. Covey *et al*., *Nat. Commun.* **7**, 11279 (2016).
99. L. D'Alessio, Y. Kafri, A. Polkovnikov, M. Rigol, *Adv. Phys.* **65**, 239–362 (2016).
100. R. Nandkishore, D. A. Huse, *Annu. Rev. Condens. Matter Phys.* **6**, 15–38 (2015).
101. L. Balents, *Nature* **464**, 199–208 (2010).
102. N. Y. Yao, M. P. Zaletel, D. M. Stamper-Kurn, A. Vishwanath, A quantum dipolar spin liquid. arXiv:1510.06403 [cond-mat.str-el] (21 October 2015).
103. N. Goldman, G. Juzeliūnas, P. Öhberg, I. B. Spielman, *Rep. Prog. Phys.* **77**, 126401 (2014).
104. J. Dalibard, F. Gerbier, G. Juzeliunas, P. Ohberg, *Rev. Mod. Phys.* **83**, 1523–1543 (2011).
105. H. Zhai, *Rep. Prog. Phys.* **78**, 026001 (2015).
106. S. V. Syzranov, M. L. Wall, V. Gurarie, A. M. Rey, *Nat. Commun.* **5**, 5391 (2014).
107. S. V. Syzranov, M. L. Wall, B. Zhu, V. Gurarie, A. M. Rey, *Nat. Commun.* **7**, 13543 (2016).
108. S. R. Manmana, E. M. Stoudenmire, K. R. A. Hazzard, A. M. Rey, A. V. Gorshkov, *Phys. Rev. B* **87**, 081106 (2013).
109. A. V. Gorshkov, K. R. A. Hazzard, A. M. Rey, *Mol. Phys.* **111**, 1908–1916 (2013).
110. N. Y. Yao *et al*., *Phys. Rev. Lett.* **109**, 266804 (2012).
111. D. Peter *et al*., *Phys. Rev. A* **91**, 053617 (2015).
112. K. A. Chao, J. Spalek, A. M. Oles, *J. Phys. C Solid State Phys.* **10**, L271–L276 (1977).
113. A. V. Gorshkov *et al*., *Phys. Rev. Lett.* **107**, 115301 (2011).
114. E. Lavert-Ofir *et al*., *Nat. Chem.* **6**, 332–335 (2014).

ACKNOWLEDGMENTS

We gratefully acknowledge many of our colleagues, both in and out of JILA, for their collaborations, discussions, and suggestions. We thank D. Reens, J. Bollinger, and R. Nandkishore for their comments on the paper. We acknowledge funding support for the work from the Army Research Office Multidisciplinary University Research Initiative (MURI), the Air Force Office of Scientific Research MURI, the Gordon and Betty Moore Foundation, the National Institute of Standards and Technology, NSF cooperative agreement PHY-1734006 supporting the JILA Physics Frontiers Center, and NSF grant PHY-1521080.

10.1126/science.aam6299

Cold molecules: Progress in quantum engineering of chemistry and quantum matter

John L. Bohn, Ana Maria Rey and Jun Ye

Science **357** (6355), 1002-1010.
DOI: 10.1126/science.aam6299